Published in final edited form as:
Plant Mol Biol. 2014 September ; 86(0): 201–214. doi:10.1007/s11103-014-0223-8.

A viable *Arabidopsis pex13* missense allele confers severe peroxisomal defects and decreases PEX5 association with peroxisomes

Andrew W. Woodward,
Department of Biochemistry and Cell Biology, Rice University, Houston, TX 77005, USA.
Department of Biology, University of Mary Hardin-Baylor, Belton, TX 76513, USA

Wendell A. Fleming,
Department of Biochemistry and Cell Biology, Rice University, Houston, TX 77005, USA

Sarah E. Burkhart,
Department of Biochemistry and Cell Biology, Rice University, Houston, TX 77005, USA

Sarah E. Ratzel,
Department of Biochemistry and Cell Biology, Rice University, Houston, TX 77005, USA

Marta Bjornson, and
Department of Biochemistry and Cell Biology, Rice University, Houston, TX 77005, USA

Bonnie Bartel
Department of Biochemistry and Cell Biology, Rice University, Houston, TX 77005, USA

Bonnie Bartel: bartel@rice.edu

Abstract

Peroxisomes are organelles that catabolize fatty acids and compartmentalize other oxidative metabolic processes in eukaryotes. Using a forward-genetic screen designed to recover severe peroxisome-defective mutants, we isolated a viable allele of the peroxisome biogenesis gene *PEX13* with striking peroxisomal defects. The *pex13-4* mutant requires an exogenous source of fixed carbon for pre-photosynthetic development and is resistant to the protoauxin indole-3-butyric acid. Delivery of peroxisome-targeted matrix proteins depends on the PEX5 receptor docking with PEX13 at the peroxisomal membrane, and we found severely reduced import of matrix proteins and less organelle-associated PEX5 in *pex13-4* seedlings. Moreover, *pex13-4* physiological and molecular defects were partially ameliorated when PEX5 was overexpressed, suggesting that PEX5 docking is partially compromised in this mutant and can be improved by increasing PEX5 levels. Because previously described *Arabidopsis pex13* alleles either are lethal

Andrew W. Woodward and Wendell A. Fleming have contributed equally to this work.

Present Address: M. Bjornson, Departments of Plant Biology and Plant Sciences, University of California, Davis, CA 95616, USA

Accession numbers

PEX13 sequences used in this article can be found in the GenBank/EMBL databases under the following accession numbers: *A. thaliana* At3g07560, *Arabidopsis lyrata* XP_002884657.1, *Nicotiana tabacum* ACB59355.1, *Oryza sativa* Os07g0152800, *Brachypodium distachyon* XP_003558114.1, *Picea sitchensis* ABK26417.1, *Selaginella moellendorffii* XP_002973297.1.

or confer only subtle defects, the *pex13-4* mutant provides valuable insight into plant peroxisome receptor docking and matrix protein import.

Keywords

Peroxisome; Organelle biogenesis; Subcellular targeting

Introduction

Peroxisomes are delimited by a single membrane and house a variety of vital metabolic reactions in plants and animals. Peroxisomes are unusual organelles in that they can divide by fission and also may derive from the endoplasmic reticulum (reviewed in Hu et al. 2012; Islinger et al. 2012). Peroxisomal metabolism is often oxidative, as in fatty acid β-oxidation, and peroxisomes also contain systems to detoxify hydrogen peroxide and other reactive oxygen species. In addition to fatty acid β-oxidation (reviewed in Graham 2008), which is essential for early *Arabidopsis* seedling establishment, plant peroxisomes sequester enzymes for the β-oxidization of precursors of auxin (reviewed in Strader and Bartel 2011) and jasmonates (reviewed in León 2013), phytohormones that are important for development and defense. In addition, plant peroxisomes house key steps in the glyoxylate cycle, photorespiration, and the biosynthesis and catabolism of various secondary metabolites (reviewed in Hu et al. 2012).

Protein import into the peroxisome matrix is unusual in that proteins—even when oligomeric or cofactor-bound—can be imported without unfolding (Glover et al. 1994; McNew and Goodman 1994; Walton et al. 1995; Lee et al. 1997). The core peroxin (PEX) proteins that mediate this remarkable import process in fungi and mammals are conserved in plants, and a framework for understanding matrix protein import exists (reviewed in Hu et al. 2012). After cytosolic translation, cargo proteins carrying a C-terminal peroxisome-targeting signal (PTS1) are recognized by the PEX5 receptor; those with an N-terminal PTS2 are recognized by PEX7. Cargo-receptor complexes dock at the peroxisome, where PEX5 insertion into the membrane allows cargo delivery to the matrix. PEX5 is then ubiquitinated and removed from the membrane with the assistance of a membrane-tethered ubiquitin-conjugating enzyme (PEX4), a complex of RING-finger ubiquitin-protein ligases (PEX2, PEX10, and PEX12), and a membrane-tethered ATPase complex (PEX1 and PEX6) (reviewed in Hu et al. 2012).

A key step in matrix protein import is docking the cargo-laden receptors at the peroxisome by the membrane peroxins PEX13 and PEX14. In several organisms, PEX14 binds both PEX5 and PEX13. A conserved PEX14 N-terminal domain binds PEX5 in yeast and mammals (reviewed in Azevedo and Schliebs 2006). However, the PEX14 regions that bind PEX13 differ between yeast and mammals (reviewed in Azevedo and Schliebs 2006). *pex13* mutants first emerged from forward-genetic screens for peroxisome dysfunction in *Pichia pastoris* (Gould et al. 1992) and *Saccharomyces cerevisiae* (Elgersma et al. 1993). Mutations in human *PEX13* (Gould et al. 1992) underlie 1–2 % of Zellweger syndrome cases (Shimozawa et al. 1999; Waterham and Ebberink 2012). Although not highly

conserved in primary sequence, PEX13 isoforms from various organisms commonly have N- and C-terminal cytosolic regions separated by two transmembrane domains that anchor the protein in the peroxisomal membrane (reviewed in Williams and Distel 2006). In humans, the PEX13 N-terminal domain is needed for homo-oligomerization and peroxisomal localization (Krause et al. 2013). In addition, the PEX13 N-terminal domain binds PEX7 in plants (Mano et al. 2006), yeast (Girzalsky et al. 1999; Stein et al. 2002), and humans (Otera et al. 2002), whereas the binding partners of the PEX13 C-terminal domain appear to be less conserved. In mammals and fungi, the PEX13 C-terminal domain includes an SH3 domain that binds PEX14 (reviewed in Williams and Distel 2006). In yeast, PEX5 also binds to the PEX13 SH3 domain, using a different binding surface than PEX14 (Douangamath et al. 2002; Pires et al. 2003). In contrast, mammalian PEX5 binds to the PEX13 N-terminal region rather than the SH3 domain (Otera et al. 2002).

In plants, docking peroxin interactions may be somewhat different from those described in other organisms. Unlike in fungi and mammals, the C-terminal region of *Arabidopsis* PEX13 lacks a recognizable SH3 domain (Boisson-Dernier et al. 2008) and binds neither peroxin nor PEX14 in yeast two-hybrid assays (Mano et al. 2006). As in other organisms, the N-terminal region of *Arabidopsis* PEX13 binds PEX7 (Mano et al. 2006), and the N-terminal region of *Arabidopsis* PEX14 binds PEX5 (Nito et al. 2002). However, *Arabidopsis* PEX13–PEX14 interactions have not been reported. Moreover, null alleles of *Arabidopsis PEX14* still allow residual matrix protein import (Hayashi et al. 2000; Monroe-Augustus et al. 2011; Burkhart et al. 2013) whereas null alleles of *Arabidopsis PEX13* confer lethality (Boisson-Dernier et al. 2008), indicating a heightened importance of PEX13 versus PEX14 in early plant development.

The isolation and characterization of viable *pex* mutants from various systems underlies our current understanding of peroxisome biogenesis and matrix protein import. Because plant peroxisomes are essential for embryonic development (reviewed in Hu et al. 2012) and gametophytic function (Boisson-Dernier et al. 2008; Li et al. 2014), partial loss-of-function alleles are necessary to interrogate the commonalities and distinctions in peroxisome biogenesis mechanisms across kingdoms. Here we describe a mutant isolated through a forward-genetic screen designed to recover severe but viable *Arabidopsis pex* alleles. The *pex13-4* missense allele displays extreme physiological impairments suggestive of β-oxidation deficiencies, a nearly complete block in matrix protein import, and less membrane-associated PEX5. Because previously described *pex13* alleles either are not viable (Boisson-Dernier et al. 2008) or only slightly reduce peroxisome function (Mano et al. 2006; Ratzel et al. 2011), *pex13-4* fills a critical gap in the mutant repertoire that will be essential for fully elucidating peroxisome biogenesis and function in plants.

Results

Isolation of a sucrose-dependent and IBA-resistant *pex13* mutant

Seedling peroxisomes convert the protoauxin indole-3-butyric acid (IBA) to the active auxin indole-3-acetic acid (IAA) (reviewed in Strader and Bartel 2011). In addition, peroxisomes are the sole site of fatty acid β-oxidation in plants (reviewed in Graham 2008). Therefore, hallmarks of seedling peroxisomal defects include resistance to IBA and dependence on

exogenous fixed carbon sources such as sucrose for growth (Zolman et al. 2000). To identify peroxisome-defective mutants, we plated progeny of mutagenized seeds on medium lacking an exogenous carbon source, discarded vigorously growing seedlings, added sucrose to the plates, and moved seedlings that commenced growth following sucrose supplementation to medium containing both sucrose and the lateral root inducer IBA. We retained seedlings that failed to produce abundant lateral roots several days after transfer to IBA as potential sucrose-dependent and IBA-resistant mutants. Recombination mapping of one such mutant localized the defect to chromosome 3 between molecular markers nga172 and MEC18 (Fig. 1a). Because this region contains *PEX13* (*At3g07560*), we sequenced *PEX13* from mutant DNA. We found a G-to-A base change at position 1,507 (relative to the initiator ATG) that resulted in a Glu243-to-Lys substitution. This amino acid change is in a C-terminal region that is highly conserved in plant PEX13 homologs (Fig. 1d). We named this new allele *pex13-4*.

To test whether the physiological defects of the *pex13-4* mutant resulted from the identified mutation, we transformed the mutant with a 2.6-kb genomic fragment that included wild-type *PEX13* coding sequences flanked by its native presumed regulatory regions. We found that this genomic clone restored sucrose independence and wild-type responses to IBA in the mutant (Fig. 1b), confirming that *pex13-4* physiological defects were due to the identified lesion in *PEX13*.

pex13-4 displays severe defects in peroxisome-related physiology

PEX13 is localized in the peroxisomal membrane (Mano et al. 2006) where it functions with PEX14 to dock the receptors PEX5 and PEX7, allowing peroxisomal cargo delivery (reviewed in Hu et al. 2012). We compared the extent of *pex13-4* defects with those of the weak *pex13-1* allele (Ratzel et al. 2011), the *pex5-1* missense allele (Zolman et al. 2000), and the null *pex14-2* allele (Monroe-Augustus et al. 2011). Wild-type seedlings convert IBA to the active auxin IAA (Zolman et al. 2000; Strader et al. 2010), resulting in short roots and hypocotyls on IBA-supplemented medium. Conversely, IBA is inefficiently converted to IAA when peroxisome function is compromised (Strader et al. 2010); *pex* mutants often elongate more robustly than wild type in the presence of IBA. As previously reported (Ratzel et al. 2011), *pex13-1* did not display IBA resistance in these assays, whereas *pex5-1* (Zolman et al. 2000) and *pex14-2* (Monroe-Augustus et al. 2011) were moderately or strongly IBA resistant, respectively (Fig. 2a, b). *pex13-4* displayed strong resistance to the inhibitory effects of IBA on root elongation in the light (Fig. 2a) and hypocotyl elongation in the dark (Fig. 2b). IBA-to-IAA conversion also increases lateral root proliferation (Zolman et al. 2000, 2001b; Strader et al. 2011; De Rybel et al. 2012), and *pex13-4* seedlings were fully resistant to IBA in this assay as well (Fig. 2e). These results suggested that *pex13-4* is more impaired in peroxisomal function than either the moderately defective *pex5-1* mutant or the severely defective *pex14-2* null mutant.

To assess fatty acid β-oxidation during early seedling development, we compared seedling growth on medium containing sucrose to growth on medium lacking an exogenous carbon source. Metabolism of seed storage oils fuels hypocotyl and root elongation in wild-type seedlings. In contrast, fatty acid β-oxidation defects in *pex14-2* seedlings reduce hypocotyl

and root elongation, which can be largely suppressed by sucrose supplementation (Monroe-Augustus et al. 2011). We found that *pex13-4* seedling growth was completely dependent on exogenous sucrose in both the light (Fig. 2c) and the dark (Fig. 2d), suggesting more severe peroxisomal defects than either *pex13-1* or *pex5-1* (Fig. 2c, d). Moreover, *pex13-4* hypocotyls and roots were shorter than wild type even when sucrose supplemented (Figs. 2a–d, 3a, b). The *pex13-4* growth defects persisted after transfer to soil, resembling the developmental delays observed in *pex14* mutants and unlike the more normal growth of *pex13-1* and *pex5-1* plants (Fig. 3c, d). These *pex13-4* growth delays were rescued by expressing wild-type *PEX13* in the mutant (Fig. 3e).

pex13-4 seedlings are defective in import of PTS1 and PTS2 proteins into peroxisomes

PEX13 works with PEX14 to dock cargo-laden PEX5 and PEX7 at the peroxisomal membrane (reviewed in Williams and Distel 2006). We used immunoblotting to examine whether levels of these peroxins were affected in the *pex13-4* mutant. We found that levels of PEX5, PEX7, and PEX14 resembled wild type in 7- and 14-day-old *pex13-4* seedlings (Fig. 4). These results suggested that PEX13 function is not needed to maintain steady-state levels of these peroxins.

Upon entry into the peroxisome, plant PTS2 proteins are processed to mature forms by removal of the PTS2-containing N-terminal peptide by the protease DEG15, a PTS1 protein (Helm et al. 2007; Schumann et al. 2008). The size difference between precursor and mature PTS2 proteins can be used to indirectly monitor PTS1 and/or PTS2 matrix protein import defects. We used immunoblotting to examine PTS2 processing of peroxisomal 3-ketoacyl-CoA thiolase (thiolase) and peroxisomal malate dehydrogenase (PMDH). Wild-type and *pex13-1* seedlings efficiently process these proteins to the mature forms (Fig. 4). In contrast, we found *pex13-4* seedling defects in PTS2 processing resembling the severe defects displayed by *pex5-1* (Fig. 4). *pex14* mutants display weaker PTS2-processing defects that become less severe as seedlings mature (Hayashi et al. 2000; Monroe-Augustus et al. 2011), whereas *pex13-4* PTS2-processing defects remained obvious even in 14-day-old seedlings (Fig. 4). Transformation with a *PEX13* genomic clone rescued the thiolase- and PMDH-processing defects of *pex13-4* (Fig. 1c), indicating that the inefficient PTS2-processing was caused by the identified mutation. The severe defects in PTS2 processing suggested that the *pex13-4* missense mutation more severely impaired matrix protein import than did the *pex14-1* nonsense mutation.

To monitor import into *pex13-4* peroxisomes directly, we used confocal microscopy to examine localization of GFP derivatives targeted to the peroxisome with a C-terminal PTS1 (Zolman and Bartel 2004) or the N-terminal PTS2-containing region from thiolase (Woodward and Bartel 2005). We found that both reporter proteins were largely cytosolic in cotyledon epidermal cells of 5-day-old *pex13-4* seedlings, in contrast to the exclusively punctate peroxisomal fluorescence observed in wild type and the presence of both cytosolic and punctate fluorescence in *pex14-1* (Fig. 5a). We used immunoblotting to examine whether our PTS2–GFP fusion protein was processed similarly to endogenous PTS2 proteins in the mutants. As expected, we observed complete processing of PTS2–GFP, native thiolase, and native PMDH in wild type and partial processing of the three proteins in

pex14-1; we observed very little processing of these proteins in *pex13-4* (Fig. 5b). We concluded that the partial loss-of-function *pex13-4* missense lesion impairs seedling matrix protein import more than the *pex14-1* lesion, even though the latter lacks detectable full-length PEX14 protein (Figs. 4, 5b) (Monroe-Augustus et al. 2011).

pex13-4 enhances other peroxin mutants

The weak *pex13* allele, *pex13-1*, enhances receptor (*pex5-1*) and docking (*pex14-2*) mutants but partially suppresses the defects of the receptor recycling mutants *pex4-1* and *pex6-1* (Ratzel et al. 2011). These observations suggest that slightly decreasing PEX5 docking can ameliorate physiological defects caused by less PEX5 recycling. To explore the impact of more severely decreasing PEX5 docking on receptor recycling mutants, we attempted to recover double mutants from crosses of *pex13-4* to receptor recycling mutants. We failed to recover viable *pex13-4 pex4-1* or *pex13-4 pex6-1* double mutants, so we crossed *pex13-4* and *pex13-1* to a weak *pex6* allele, *pex6-2* (Burkhart et al. 2013). We then compared the physiological and molecular consequences of slightly (*pex13-1*) or substantially (*pex13-4*) reducing PEX13 function in *pex6-2*. We assessed peroxisome function in the mutants by monitoring processing of PTS2 proteins, comparing growth with and without sucrose, and examining response to the IBA analog 2,4-dichlorophenoxybutyric acid (2,4-DB), which is processed to the synthetic auxin 2,4-dichlorophenoxy-acetic acid in peroxisomes (Hayashi et al. 1998). Like *pex6-1* (Ratzel et al. 2011), we found that *pex13-1* significantly ameliorated the physiological defect (2,4-DB resistance) of *pex6-2* (Fig. 6a). In addition, the slight thiolase-processing defect of *pex6-2* was no longer apparent in the *pex13-1 pex6-2* double mutant (Fig. 6b). In contrast, the *pex13-4 pex6-2* double mutant resembled *pex13-4*, showing complete sucrose dependence and 2,4-DB resistance in the dark (Fig. 6a) and severe PTS2-processing defects of both thiolase and PMDH (Fig. 6b). The slight enhancement of *pex13-4* PTS2-processing defects by *pex6-2* (Fig. 6b) and the apparent lethality that resulted from combining *pex13-4* with *pex6-1* or *pex4-1* are consistent with the possibility that matrix protein import is not completely abrogated in *pex13-4*.

PEX5 is less peroxisome associated in *pex13-4*

Because PEX13 functions in fungi and animals to dock PEX5 at the peroxisomal membrane to allow cargo delivery (reviewed in Williams and Distel 2006), we examined PEX5 distribution in wild-type and mutant seedlings. We used centrifugation to fractionate seedling homogenates, separating soluble fractions containing cytosol from pellet fractions containing organellar membranes. We monitored the effectiveness of the fractionation by probing immunoblots with antibodies to a mitochondrial membrane ATP synthase, which was predominantly confined to the pellet fractions in all lines (Fig. 7). We developed an antibody to the C-terminal domain of PEX13, and found that wild-type PEX13 appeared as single ~34-kDa band (similar to the predicted 31 kDa molecular mass of *Arabidopsis* PEX13) and pex13-4 protein appeared as an approximately 34-kDa doublet on immunoblots (Fig. 7). PEX13 was restricted to the pellet fraction in wild type (Fig. 7), as expected for a peroxisomal membrane protein (Mano et al. 2006). The *pex13-4* lesion did not affect membrane association of the mutant protein; PEX13 remained organelle-associated in both *pex13* alleles and in *pex14-1* (Fig. 7). Similarly, we found that the other docking peroxin, PEX14, was largely in the pellet fraction in wild type and in both *pex13* mutants, implying

that PEX14 does not require PEX13 function for membrane association or stability. The distribution of PEX7 protein among the soluble, wash, and organellar fractions in wild type and the mutants was similar (Fig. 7) and suggested that the majority of PEX7 is cytosolic in all the assayed lines. As previously reported (Ratzel et al. 2011), we found PEX5 in both pellet and soluble fractions prepared from wild-type and *pex13-1* seedling extracts (Fig. 7). We found a greater fraction of soluble versus organelle-associated PEX5 in *pex13-4* extracts (Fig. 7). The *pex14-1* fractionation revealed an intermediate defect in PEX5 localization between wild type and *pex13-4* (Fig. 7), consistent with the intermediate matrix protein mislocalization phenotype of *pex14-1* (Fig. 5a). Our fractionation results suggest that PEX5 insertion in the peroxisomal membrane is impaired in the *pex13-4* mutant, consistent with a role for PEX13 in docking PEX5 at the peroxisome or inserting PEX5 into the peroxisomal membrane.

Overexpressing *PEX5* partially ameliorates some *pex13-4* mutant defects

Because we observed that PEX5 was less associated with organelles in the *pex13-4* mutant (Fig. 7), we examined whether *PEX5* overexpression could offset the negative consequences of the *pex13-4* lesion. Overexpressing *PEX5* in an otherwise wild-type background was slightly detrimental, conferring minor PTS2-processing defects (Fig. 8a) and slight IBA resistance (Fig. 8b, c). As previously reported (Zolman and Bartel 2004; Burkhart et al. 2013), overexpressing *PEX5* partially ameliorated *pex6-1* PTS2-processing defects (Fig. 8a) and sucrose dependence but did not notably counter *pex6-1* IBA resistance in either light- (Fig. 8b) or dark-grown (Fig. 8c) seedlings. We found that increasing PEX5 levels in *pex13-4* reduced the PTS2-processing defects (Fig. 8a) and slightly reduced the dependence of seedlings on sucrose for growth in the light (Fig. 8b). Moreover, increasing PEX5 levels partially countered *pex13-4* elongation defects on unsupplemented medium (Fig. 8c, e) and decreased the relative IBA resistance of *pex13-4* seedlings in root (Fig. 8b) and hypocotyl (Fig. 8c) elongation. However, PEX5 overexpression did not restore all *pex13-4* defects; *pex13-4 35S:PEX5* seedlings remained fully dependent on sucrose for hypocotyl elongation in the dark (Fig. 8c) and failed to produce lateral roots in response to IBA (Fig. 8d). The partial amelioration of peroxisomal defects by *PEX5* overexpression suggests that PEX5 function is limiting in the *pex13-4* mutant and that the pex13-4 protein that remains present in the mutant (Fig. 7) retains partial function.

Discussion

Including *pex13-4*, four *Arabidopsis pex13* alleles of varying severity have been reported (Fig. 1d). The *pex13-1* T-DNA insertion upstream of the *PEX13* start codon decreases *PEX13* mRNA levels and modifies defects of other *pex* mutants, but lacks dramatic defects as a single mutant (Ratzel et al. 2011). Similarly, PEX13 function is only slightly impaired by the truncation encoded by *aberrant peroxisome morphology2* (*apm2*), which lacks the final 42 amino acids of PEX13 (Fig. 1d) but displays only slight import defects accompanied by nearly normal β-oxidation (Mano et al. 2006). At the opposite end of the spectrum, the *abstinence by mutual consent* (*amc*) allele harbors a T-DNA in the third exon of *PEX13* (Fig. 1d) and displays gametophytic defects that preclude viability—and thus analysis—as a homozygote (Boisson-Dernier et al. 2008). *pex13-4* is a missense allele (Fig. 1) that largely

prevents peroxisomal matrix protein import (Fig. 5) and confers dramatic IBA resistance and complete dependence on sucrose for seedling establishment (Fig. 2). The severe physiological and molecular defects of the viable *pex13-4* mutant appear similar to those reported following RNAi-mediated reduction of *PEX13* (Nito et al. 2007); *pex13-4* thus represents a valuable tool with which to address PEX13 function in plants.

The previously characterized *pex13-1* mutant enhances defects of mutants defective in the PEX5 receptor or the PEX14 docking peroxin and partially suppresses defects of the *pex4-1* and *pex6-1* receptor recycling mutants (Ratzel et al. 2011). In contrast, the apparent lethality of *pex13-4 pex4-1* and *pex13-4 pex6-1* double mutants implies that the *pex13-4* mutation enhances, rather than suppresses, receptor-recycling defects presumed to underlie *pex4* and *pex6* mutant phenotypes. To validate this conclusion, we compared the genetic interactions of *pex13-1* and *pex13-4* with a weak *pex6* allele, *pex6-2* (Burkhart et al. 2013). As with *pex4-1* and *pex6-1* (Ratzel et al. 2011), *pex13-1* suppressed the *pex6-2* β-oxidation and PTS2-processing defects (Fig. 6). In contrast, the PTS2-processing defects of *pex13-4 pex6-2* were at least as severe as those of *pex13-4* (Fig. 6b).

The consequences of PEX5 overexpression provide mechanistic insights into the molecular basis of *pex* mutant defects. For example, PEX5 overexpression ameliorates certain *pex6-1* defects, suggesting that the low PEX5 levels observed in this mutant limit matrix protein import (Zolman and Bartel 2004; Burkhart et al. 2013). In contrast, PEX5 overexpression confers slight peroxisomal defects in wild type (Fig. 8), indicating that excess PEX5 can be detrimental. The improved PTS2 processing and peroxisome-related physiology upon PEX5 overexpression in *pex13-4* (Fig. 8) are consistent with the idea that the *pex13-4* mutant defects are caused by decreased peroxisomal matrix protein import resulting from reduced association of PEX5 with *pex13-4* peroxisomes (Fig. 7).

pex13-4 was isolated in a two-part screen designed to recover severe peroxin alleles. Our previous screens for peroxisomal defects relied on robust root elongation on IBA concentrations that inhibit root elongation in wild type (Zolman et al. 2000). A variety of *pex* alleles were recovered from this root elongation-based screen, including *pex4-1* (Zolman et al. 2005), *pex5-1* (Zolman et al. 2000), *pex6-1* (Zolman and Bartel 2004), *pex7-2* (Ramón and Bartel 2010), and *pex14-1* (Monroe-Augustus et al. 2011). At the same time, IBA-resistance screens also recovered mutants defective in enzymes that directly or indirectly promote IBA-to-IAA conversion (Zolman et al. 2001a; Adham et al. 2005; Zolman et al. 2007, 2008; Strader et al. 2011), some of which were recovered at a high frequency (Zolman et al. 2001a, 2007). Similarly, screens for 2,4-DB resistance (Hayashi et al. 1998, 2000) or sucrose dependence (Eastmond 2006, 2007) yield not only *pex* mutants but also mutants defective in fatty acid-utilization enzymes. In this study, by requiring both sucrose dependence and IBA resistance in the primary screen, we aimed to avoid mutations in genes encoding IBA-to-IAA conversion enzymes while increasing the recovery of severe *pex* alleles. Indeed, *pex13-4* displays the most severe peroxisomal defects of any *pex* mutant we have recovered using forward genetics. However, this screen still allows recovery of mutants defective in proteins needed for β-oxidation of both IBA and fatty acids, such as the PXA1 transporter that brings both compounds into peroxisomes (Zolman et al. 2001b) and

the thiolase isozyme that catalyzes the last step of β-oxidation (Hayashi et al. 1998; Lingard and Bartel 2009).

The *pex13-4* missense allele alters a Glu residue in the C-terminal domain that is conserved in various plant PEX13 homologs (Fig. 1d). In fungi and mammals, the C-terminal region of PEX13 extends from the peroxisomal membrane into the cytosol and contains an SH3 domain (reviewed in Williams and Distel 2006). The SH3 domain is the site of causal mutations in several individuals affected by Zellweger syndrome (Liu et al. 1999; Shimozawa et al. 1999; Krause et al. 2013). Like *Arabidopsis pex13-4* (Fig. 5), some mammalian SH3-domain mutations impair both PTS1 and PTS2 import (Liu et al. 1999; Toyama et al. 1999). In contrast, the human Trp313Gly substitution in the PEX13 SH3 domain impairs PTS1 but not PTS2 import (Krause et al. 2013). In yeast, the PEX13 SH3 domain binds PEX14 and PEX5 on different surfaces (Douangamath et al. 2002; Pires et al. 2003). Although a similar SH3 domain is not apparent in the primary sequence of *Arabidopsis* PEX13 (Boisson-Dernier et al. 2008), and although various segments of *Arabidopsis* PEX13, including the C-terminal 94 or 158 amino acids, do not bind PEX14 or PEX5 in yeast two-hybrid assays (Mano et al. 2006), we cannot exclude the possibility that this region binds PEX14 and/or PEX5 in vivo.

Interestingly, the *pex13-4* Glu243Lys substitution is only 20 residues upstream of the *apm2* nonsense mutation (Fig. 1d) that confers much weaker peroxisomal defects than *pex13-4* (Mano et al. 2006). Together, the severe physiological and molecular defects conferred by the *pex13-4* missense mutation and the conservation of the C-terminal region among diverse plants (Fig. 1d) suggest that structural and interaction studies with the *Arabidopsis* PEX13 C-terminal domain will assist in uncovering the molecular roles of this critical docking peroxin in plants.

Among the core peroxins that facilitate matrix protein import, PEX13, PEX22, and PEX26/PEX15/APEM9 are particularly poorly conserved among kingdoms compared to the matrix protein receptors (PEX5 and PEX7) or peroxins with enzymatic activities (the PEX4 ubiquitin-conjugating enzyme, the PEX2, PEX10, and PEX12 ubiquitin-protein ligases, and the PEX1 and PEX6 ATPases) (Mullen et al. 2001). Despite lacking primary sequence similarity, *Arabidopsis* PEX22 and PEX26/PEX15/APEM9 appear to function similarly to their fungal counterparts to tether PEX4 and PEX1–PEX6, respectively, to the peroxisomal membrane (Zolman et al. 2005; Goto et al. 2011). A lack of conservation might be rationalized by the relatively simple tethering functions of PEX22 and PEX26/PEX15. Similarly, the weak evolutionary conservation of PEX13 might reflect a relatively simple function of bringing the receptors into proximity with the peroxisomal membrane. Conversely, the divergence of PEX13 sequences among kingdoms might reflect altered functions, as hinted by the failure to detect interactions among the *Arabidopsis* peroxins for which the yeast or mammalian counterparts interact (Mano et al. 2006). The characterization of the *pex13-4* allele supports a model in which PEX13 promotes peroxisomal membrane association of the PEX5 receptor protein, which is necessary for peroxisome function. Future analyses using this viable allele with easily assayed phenotypes will enable characterization of the critical receptor docking process in plants.

Methods

Plant materials and growth conditions

All mutants were in the *Arabidopsis thaliana* Col-0 accession. For phenotypic assays, seeds were surface sterilized in 30 % [v/v] bleach, 0.01 % [v/v] Triton X-100, stratified 1–3 days at 4 °C, and plated on plant nutrient medium (PN) (Haughn and Somerville 1986) solidified with 0.6 % [w/v] agar and supplemented with 0.5 % [w/v] sucrose (PNS) and ethanol-dissolved hormone stock solutions as indicated, and incubated at 22 °C in continuous light or darkness as indicated. For experiments using IBA or 2,4-DB, light was filtered with yellow long-pass filters to slow breakdown of indolic compounds (Stasinopoulos and Hangarter 1990). For lateral-root assays, seedlings were stratified for 1 day and then grown under yellow-filtered light on PNS for 4 days followed by 4 days on PNS containing 10 μM IBA or the equivalent amount of ethanol.

The *pex13-4* mutant was isolated in a screen for sucrose-dependent and IBA-resistant seedlings. Approximately 156,000 seeds from 26 separately pooled M_2 progeny of Col-0 seeds treated with 0.24 % [v/v] ethyl methanesulfonate for 16 h were surface sterilized, plated on 150-mm PN plates, and incubated in light for 3–6 h before wrapping in foil and incubating in darkness for 5 days at 22 °C, at which time seedlings with >1-mm hypocotyls were removed using a forceps and discarded. 2 mL 50 % [w/v] sucrose solution was added to each plate (to a final concentration of 1 % [w/v]). Plates were resealed with gas-permeable tape and incubated in white light for an additional 7 days at 22 °C. Seedlings that developed in the presence of sucrose were transferred to PNS plates supplemented with 10 μM IBA. Plates were incubated in yellow light at 22 °C for an additional 5 days, and seedlings that produced few lateral roots in the presence of IBA were transferred to a PNS plate and grown for a few more days before transfer to soil for seed production.

For recombination mapping of the *pex13-4* lesion, DNA was isolated from sucrose-dependent, IBA-resistant plants selected from F_2 progeny of *pex13-4* crossed to the Wassilewskija (Ws) accession. Mapping with PCR-based molecular markers was used to localize the causal lesion to a region near the top of chromosome 3. The *PEX13* (*At3g07560*) gene was PCR-amplified from genomic DNA prepared from the mutant, and PCR amplicons were sequenced directly (Lone Star Labs, Houston, TX) with the primers used for amplification.

pex13-4 was backcrossed to the parental Col-0 accession twice before phenotypic assays. The *pex13-4* mutant was identified in segregating populations using a derived Cleaved Amplified Polymorphic Sequence (dCAPS) marker (Michaels and Amasino 1998; Neff et al. 1998). Amplification with PEX13-19 (5′-CTTATAGATCAAAACACACAGGCCTTTCACATG-3′) and PEX13-*Hinf*I (5′-AAGCATACGCAGTACAAATCTTGCTGATT-3′; altered residue underlined) yielded a 211-bp product. Digestion of this amplicon with *Hinf*I resulted in a 180-bp fragment for wild-type *PEX13*, whereas the *pex13-4* fragment was not cleaved. The genotypes of *pex4-1* (Zolman et al. 2005), *pex5-1* (Zolman et al. 2000), *pex6-1* (Zolman and Bartel 2004), *pex6-2* (Burkhart et al. 2013), *pex7-1* (Woodward and Bartel 2005), *pex13-1* (Ratzel et al. 2011),

pex14-1 (Monroe-Augustus et al. 2011), and *pex14-2* (Monroe-Augustus et al. 2011) were assayed as described previously.

To obtain *pex13-4* overexpressing PEX5, *pex13-4* was crossed to *pex6-1* transformed with *35S:PEX5*, which drives a *PEX5* cDNA from the cauliflower mosaic virus *35S* promoter (Zolman and Bartel 2004), and plants homozygous for *pex13-4* and *35S:PEX5* and carrying two wild-type *PEX6* alleles were obtained from the progeny. Wild-type Col-0 overexpressing *PEX5* was similarly obtained after crossing *pex6-1* (*35S:PEX5*) (Zolman and Bartel 2004) to wild type. Plants carrying the *35S:PEX5* transgene were identified by PCR amplification with *PEX5* primers PEX5-38 (5′-TGAAGACCAACAGATAAGG-3′) and PEX5-39 (5′-CCCATTGGAGGCATAGG-3′), which annealed to different exons and amplified a 168-bp product from the transgene and a 264-bp product from the genomic *PEX5* locus.

DNA methods

For the *pex13-4* rescue construct, the *PEX13* genomic region was PCR amplified using Platinum *Pfx* polymerase (Invitrogen) from wild-type Col-0 genomic DNA using 1891-PEX13 (5′-CACCCGCGCTCGCCGCCATTAAATACCCAATTT-3′; underlined sequence was appended to confer directionality to Gateway cloning) and 1843-PEX13 (5′-AATGTGTTGGTCTTGTCTAGAGGCAAACT-3′). The resultant 2,643-bp amplicon included 527 bp of DNA upstream of the *PEX13* start codon, the *PEX13* coding sequence, and 417 bp downstream of the *PEX13* stop codon. This fragment was cloned using the Gateway system into pENTR/D-TOPO (Invitrogen), sequenced to confirm that no mutations were introduced during amplification, and recombined into the destination vector pMDC100 (Curtis and Grossniklaus 2003) to give pMDC100-*PEX13*. pMDC100-*PEX13* was electroporated into *Agrobacterium tumefaciens* GV3101 (Koncz and Schell 1986), which was used to transform *pex13-4* plants using the floral dip method (Clough and Bent 1998). Transformants were selected on PN medium containing 15 μg/mL kanamycin (selecting for both restored sucrose independence and kanamycin resistance), and progeny were selected on PNS medium containing 15 μg/mL kanamycin. Homozygous progeny from two independent transformants were used for phenotypic assays.

Immunoblot analysis

Protein was extracted from seedlings grown on PNS under continuous light for the indicated number of days by grinding frozen tissue and mixing with two volumes 2× NuPAGE loading buffer (Invitrogen, Carlsbad, CA). After centrifugation, the supernatant was transferred to a fresh tube, dithiothreitol was added to 50 mM from a 500 mM stock, and samples were heated at 100 °C for 5 min. Samples were loaded onto NuPAGE 10 % Bis–Tris gels (Invitrogen) alongside prestained protein markers (P7708S, New England Biolabs, Beverly, MA) and Cruz Markers (sc-2035, Santa Cruz Biotechnology, Santa Cruz, CA). After electrophoresis using NuPAGE MOPS-SDS running buffer (Invitrogen), proteins were transferred for 30–35 min at 24 V to a Hybond ECL nitrocellulose membrane (Amersham Pharmacia Biotech, Piscataway, NJ) using NuPAGE transfer buffer (Invitrogen). Membranes were blocked at 4 °C with 8 % [w/v] non-fat dry milk in TBST [Tris-buffered saline with 0.1 % [v/v] Tween-20 (Ausubel et al. 1999)], and incubated overnight at 4 °C

with the following primary antibodies diluted in blocking buffer: rabbit anti-PEX5 (1:100 dilution, Zolman and Bartel 2004), rabbit anti-PEX7 (1:2,000 dilution, Ramón and Bartel 2010), rabbit anti-PEX13 (1:100, prepared from rabbits inoculated with a recombinant protein including amino acids 215–304 of PEX13), rabbit anti-PEX14 (1:10,000 dilution, Agrisera AS08 or Lingard and Bartel 2009), rabbit anti-thiolase (1:2,500 dilution, Lingard et al. 2009), rabbit anti-PMDH2 (1:2,000 dilution, Pracharoenwattana et al. 2007), mouse anti-GFP (1:200 dilution, sc-9996, Santa Cruz Biotechnology), mouse α-mitochondrial ATP synthase (1:2,000, MitoScience MS507), or mouse anti-HSC70 (1:20,000–1:100,000 dilution, SPA-817, StressGen Biotechnologies). Horseradish peroxidase (HRP)-linked goat anti-rabbit or anti-mouse IgG (sc-2030 or sc-2031, Santa Cruz Biotechnology) were used as secondary antibodies and were visualized using WesternBright ECL HRP substrate (Advansta, Menlo Park, CA) detected using autoradiography film. Membranes were reblocked and sequentially probed with the indicated antibodies without stripping the membrane between incubations. Immunoblot experiments were repeated at least twice with similar results.

Cell fractionation

Organelles were separated from cytosol as previously described (Ratzel et al. 2011): 8-day-old light-grown seedlings (from 5 mg of dry seed) were chopped with scissors in 1 mL ice-cold fractionation buffer [150 mM Tris pH 7.6, 100 mM sucrose, 10 mM KCl, 1 mM EDTA, 1 mM dithiothreitol, 1 mM *N*-ethylmaleimide, 1× protease inhibitor cocktail (P9559, Sigma)], homogenized (20 strokes) with a Dounce homogenizer, filtered through Miracloth (Millipore), and centrifuged for 10 min at 640 rpm to remove cellular debris, giving a homogenate fraction. The volume of the homogenate (generally ~200 μL) was noted, and the homogenate was centrifuged for 20 min at 12,000 rpm to give the supernatant fraction. The pellet was washed once with a volume of fractionation buffer equal to the homogenate volume, centrifuged for 20 min at 12,000 rpm to give a wash fraction, and suspended in a volume of fractionation buffer equal to the homogenate volume to give the pellet fraction. Following fractionation, an aliquot of each fraction was mixed with an equal volume of NuPAGE 2× loading buffer (Invitrogen) and 25 μL samples were processed for sequential immunoblotting as described above.

Confocal microscopy

Wild-type Col-0 lines transformed with *35S:GFP–PTS1* (Zolman and Bartel 2004) or *35S:PTS2–GFP* (Woodward and Bartel 2005) crossed with *pex14-1* were previously described (Monroe-Augustus et al. 2011). *pex13-4* was similarly crossed to wild type carrying *35S:GFP–PTS1* or *35S:PTS2–GFP*. Cotyledon epidermal cells of 5-day-old light-grown seedlings were mounted in water, and images were collected using a Carl Zeiss LSM 710 laser scanning confocal microscope equipped with a Meta detector. Samples were imaged using a 40× oil immersion objective following excitation with a 488-nm argon laser. GFP emission was collected between 494 and 560 nm. Each image is an average of 16 exposures using a 54-μm pinhole, corresponding to a 1.6-μm optical slice.

Statistical analysis

The SPSS Statistics software (version 21.0.0.1) was used to analyze statistical significance of measurements using one-way analysis of variance (ANOVA) followed by Duncan's test.

Acknowledgments

We thank Steven Smith (University of Western Australia) for the PMDH2 antibody, Monique Gill for assistance with the mutant screen, and Kim Gonzalez, Yun-Ting Kao, Mauro Rinaldi, and Pierce Young for critical comments on the manuscript. This research was supported by the National Science Foundation (MCB-1244182) and the Robert A. Welch Foundation (C-1309). Confocal microscopy was performed on equipment obtained through a Shared Instrumentation Grant from the National Institutes of Health (S10RR026399). A. W. W. was partially supported by a UMHB Faculty Development Grant, and M. B. was partially supported by a Howard Hughes Medical Institute Professors Grant (52005717 to B. B.).

References

Adham AR, Zolman BK, Millius A, Bartel B. Mutations in *Arabidopsis* acyl-CoA oxidase genes reveal distinct and overlapping roles in β-oxidation. Plant J. 2005; 41:859–874. [PubMed: 15743450]

Ausubel, F.; Brent, R.; Kingston, RE.; Moore, DD.; Seidman, JG.; Smith, JA.; Struhl, K. Current protocols in molecular biology. Greene Publishing Associates and Wiley-Interscience; New York: 1999.

Azevedo JE, Schliebs W. Pex14p, more than just a docking protein. Biochim Biophys Acta. 2006; 1763:1574–1584. [PubMed: 17046076]

Boisson-Dernier A, Frietsch S, Kim T-H, Dizon MB, Schroeder JI. The peroxin loss-of-function mutation *abstinence by mutual consent* disrupts recognition between male and female gametophytes. Curr Biol. 2008; 18:63–68. [PubMed: 18160292]

Burkhart SE, Lingard MJ, Bartel B. Genetic dissection of peroxisome-associated matrix protein degradation in *Arabidopsis thaliana*. Genetics. 2013; 193:125–141. [PubMed: 23150599]

Clough SJ, Bent AF. Floral dip: a simplified method for *Agrobacterium*-mediated transformation of *Arabidopsis thaliana*. Plant J. 1998; 16:735–743. [PubMed: 10069079]

Curtis MD, Grossniklaus U. A gateway cloning vector set for high-throughput functional analysis of genes *in planta*. Plant Physiol. 2003; 133:462–469. [PubMed: 14555774]

De Rybel B, Audenaert D, Xuan W, Overvoorde P, Strader LC, Kepinski S, Hoye R, Brisbois R, Parizot B, Vanneste S, Liu X, Gilday A, Graham IA, Nguyen L, Jansen L, Njo MF, Inze D, Bartel B, Beeckman T. A role for the root cap in root branching revealed by the non-auxin probe naxillin. Nat Chem Biol. 2012; 8:798–805. [PubMed: 22885787]

Douangamath A, Filipp FV, Klein AT, Barnett P, Zou P, Voorn-Brouwer T, Vega MC, Mayans OM, Sattler M, Distel B, Wilmanns M. Topography for independent binding of alpha-helical and PPII-helical ligands to a peroxisomal SH3 domain. Mol Cell. 2002; 10:1007–1017. [PubMed: 12453410]

Eastmond PJ. *SUGAR-DEPENDENT1* encodes a patatin domain triacylglycerol lipase that initiates storage oil breakdown in germinating *Arabidopsis* seeds. Plant Cell. 2006; 18:665–675. [PubMed: 16473965]

Eastmond PJ. *MONODEHYROASCORBATE REDUCTASE4* is required for seed storage oil hydrolysis and postgerminative growth in *Arabidopsis*. Plant Cell. 2007; 19:1376–1387. [PubMed: 17449810]

Elgersma Y, van den Berg M, Tabak HF, Distel B. An efficient positive selection procedure for the isolation of peroxisomal import and peroxisome assembly mutants of *Saccharomyces cerevisiae*. Genetics. 1993; 135:731–740. [PubMed: 7507454]

Girzalsky W, Rehling P, Stein K, Kipper J, Blank L, Kunau W-H, Erdmann R. Involvement of Pex13p in Pex14p localization and peroxisomal targeting signal 2-dependent protein import into peroxisomes. J Cell Biol. 1999; 144:1151–1162. [PubMed: 10087260]

Glover JR, Andrews DW, Rachubinski RA. *Saccharomyces cerevisiae* peroxisomal thiolase is imported as a dimer. Proc Natl Acad Sci USA. 1994; 91:10541–10545. [PubMed: 7937990]

Goto S, Mano S, Nakamori C, Nishimura M. *Arabidopsis* ABERRANT PEROXISOME MORPHOLOGY9 is a peroxin that recruits the PEX1–PEX6 complex to peroxisomes. Plant Cell. 2011; 23:1573–1587. [PubMed: 21487094]

Gould SJ, McCollum D, Spong AP, Heyman JA, Subramani S. Development of the yeast *Pichia pastoris* as a model organism for a genetic and molecular analysis of peroxisome assembly. Yeast. 1992; 8:613–628. [PubMed: 1441741]

Graham IA. Seed storage oil mobilization. Annu Rev Plant Biol. 2008; 59:115–142. [PubMed: 18444898]

Haughn GW, Somerville C. Sulfonylurea-resistant mutants of *Arabidopsis thaliana*. Mol Gen Genet. 1986; 204:430–434.

Hayashi M, Toriyama K, Kondo M, Nishimura M. 2,4-Dichlorophenoxybutyric acid-resistant mutants of *Arabidopsis* have defects in glyoxysomal fatty acid β-oxidation. Plant Cell. 1998; 10:183–195. [PubMed: 9490742]

Hayashi M, Nito K, Toriyama-Kato K, Kondo M, Yamaya T, Nishimura M. AtPex14p maintains peroxisomal functions by determining protein targeting to three kinds of plant peroxisomes. EMBO J. 2000; 19:5701–5710. [PubMed: 11060021]

Helm M, Lück C, Prestele J, Hierl G, Huesgen PF, Frohlich T, Arnold GJ, Adamska I, Görg A, Lottspeich F, Gietl C. Dual specificities of the glyoxysomal/peroxisomal processing protease DEG15 in higher plants. Proc Natl Acad Sci USA. 2007; 104:11501–11506. [PubMed: 17592111]

Hu J, Baker A, Bartel B, Linka N, Mullen RT, Reumann S, Zolman BK. Plant peroxisomes: biogenesis and function. Plant Cell. 2012; 24:2279–2303. [PubMed: 22669882]

Islinger M, Grille S, Fahimi HD, Schrader M. The peroxisome: an update on mysteries. Histochem Cell Biol. 2012; 137:547–574. [PubMed: 22415027]

Koncz C, Schell J. The promoter of the T_L-DNA gene 5 controls the tissue-specific expression of chimaeric genes carried by a novel type of *Agrobacterium* binary vector. Mol Gen Genet. 1986; 204:383–396.

Krause C, Rosewich H, Woehler A, Gartner J. Functional analysis of PEX13 mutation in a Zellweger syndrome spectrum patient reveals novel homooligomerization of PEX13 and its role in human peroxisome biogenesis. Hum Mol Genet. 2013; 22:3844–3857. [PubMed: 23716570]

Lee MS, Mullen RT, Trelease RN. Oilseed isocitrate lyases lacking their essential type 1 peroxisomal targeting signal are piggybacked to glyoxysomes. Plant Cell. 1997; 9:185–197. [PubMed: 9061950]

León J. Role of plant peroxisomes in the production of jasmonic acid-based signals. Subcell Biochem. 2013; 69:299–313. [PubMed: 23821155]

Li XR, Li HJ, Yuan L, Liu M, Shi DQ, Liu J, Yang WC. *Arabidopsis* DAYU/ABERRANT PEROXISOME MORPHOLOGY9 is a key regulator of peroxisome biogenesis and plays critical roles during pollen maturation and germination in planta. Plant Cell. 2014; 26:619–635. [PubMed: 24510720]

Lingard MJ, Bartel B. *Arabidopsis* LON2 is necessary for peroxisomal function and sustained matrix protein import. Plant Physiol. 2009; 151:1354–1365. [PubMed: 19748917]

Lingard MJ, Monroe-Augustus M, Bartel B. Peroxisome-associated matrix protein degradation in *Arabidopsis*. Proc Natl Acad Sci USA. 2009; 106:4561–4566. [PubMed: 19246395]

Liu Y, Björkman J, Urquhart A, Wanders RJA, Crane DI, Gould SJ. *PEX13* is mutated in complementation group 13 of the peroxisome-biogenesis disorders. Am J Hum Genet. 1999; 65:621–634. [PubMed: 10441568]

Mano S, Nakamori C, Nito K, Kondo M, Nishimura M. The *Arabidopsis pex12* and *pex13* mutants are defective in both PTS1- and PTS2-dependent protein transport to peroxisomes. Plant J. 2006; 47:604–618. [PubMed: 16813573]

McNew JA, Goodman JM. An oligomeric protein is imported into peroxisomes in vivo. J Cell Biol. 1994; 127:1245–1257. [PubMed: 7962087]

Michaels SD, Amasino RM. A robust method for detecting single-nucleotide changes as polymorphic markers by PCR. Plant J. 1998; 14:381–385. [PubMed: 9628032]

Monroe-Augustus M, Ramón NM, Ratzel SE, Lingard MJ, Christensen SE, Murali C, Bartel B. Matrix proteins are inefficiently imported into *Arabidopsis* peroxisomes lacking the receptor-docking peroxin PEX14. Plant Mol Biol. 2011; 77:1–15. [PubMed: 21553312]

Mullen RT, Flynn CR, Trelease RN. How are peroxisomes formed? The role of the endoplasmic reticulum and peroxins. Trends Plant Sci. 2001; 6:256–261. [PubMed: 11378467]

Neff MM, Neff JD, Chory J, Pepper AE. dCAPS, a simple technique for the genetic analysis of single nucleotide polymorphisms: experimental applications in *Arabidopsis thaliana* genetics. Plant J. 1998; 14:387–392. [PubMed: 9628033]

Nito K, Hayashi M, Nishimura M. Direct interaction and determination of binding domains among peroxisomal import factors in *Arabidopsis thaliana*. Plant Cell Physiol. 2002; 43:355–366. [PubMed: 11978862]

Nito K, Kamigaki A, Kondo M, Hayashi M, Nishimura M. Functional classification of *Arabidopsis* peroxisome biogenesis factors proposed from analyses of knockdown mutants. Plant Cell Physiol. 2007; 48:763–774. [PubMed: 17478547]

Otera H, Setoguchi K, Hamasaki M, Kumashiro T, Shimizu N, Fujiki Y. Peroxisomal targeting signal receptor Pex5p interacts with cargoes and import machinery components in a spatiotemporally differentiated manner: conserved Pex5p WXXXF/Y motifs are critical for matrix protein import. Mol Cell Biol. 2002; 22:1639–1655. [PubMed: 11865044]

Pires JR, Hong X, Brockmann C, Volkmer-Engert R, Schneider-Mergener J, Oschkinat H, Erdmann R. The ScPex13p SH3 domain exposes two distinct binding sites for Pex5p and Pex14p. J Mol Biol. 2003; 326:1427–1435. [PubMed: 12595255]

Pracharoenwattana I, Cornah JE, Smith SM. *Arabidopsis* peroxisomal malate dehydrogenase functions in β-oxidation but not in the glyoxylate cycle. Plant J. 2007; 50:381–390. [PubMed: 17376163]

Ramón NM, Bartel B. Interdependence of the peroxisome-targeting receptors in *Arabidopsis thaliana*: PEX7 facilitates PEX5 accumulation and import of PTS1 cargo into peroxisomes. Mol Biol Cell. 2010; 21:1263–1271. [PubMed: 20130089]

Ratzel SE, Lingard MJ, Woodward AW, Bartel B. Reducing *PEX13* expression ameliorates physiological defects of late-acting peroxin mutants. Traffic. 2011; 12:121–134. [PubMed: 20969679]

Schumann H, Huesgen PF, Gietl C, Adamska I. The DEG15 serine protease cleaves peroxisomal targeting signal 2-containing proteins in *Arabidopsis*. Plant J. 2008; 148:1847–1856.

Shimozawa N, Suzuki Y, Zhang Z, Imamura A, Toyama R, Mukai S, Fujiki Y, Tsukamoto T, Osumi T, Orii T, Wanders RJ, Kondo N. Nonsense and temperature-sensitive mutations in PEX13 are the cause of complementation group H of peroxisome biogenesis disorders. Hum Mol Genet. 1999; 8:1077–1083. [PubMed: 10332040]

Stasinopoulos TC, Hangarter RP. Preventing photochemistry in culture media by long-pass light filters alters growth of cultured tissues. Plant Physiol. 1990; 93:1365–1369. [PubMed: 16667626]

Stein K, Schell-Steven A, Erdmann R, Rottensteiner H. Interactions of Pex7p and Pex18p/Pex21p with the peroxisomal docking machinery: implications for the first steps in PTS2 protein import. Mol Cell Biol. 2002; 22:6056–6069. [PubMed: 12167700]

Strader LC, Bartel B. Transport and metabolism of the endogenous auxin precursor indole-3-butyric acid. Mol Plant. 2011; 4:477–486. [PubMed: 21357648]

Strader L, Culler Hendrickson A, Cohen J, Bartel B. Conversion of endogenous indole-3-butyric acid to indole-3-acetic acid drives cell expansion in *Arabidopsis* seedlings. Plant Physiol. 2010; 153:1577–1586. [PubMed: 20562230]

Strader LC, Wheeler DL, Christensen SE, Berens JC, Cohen JD, Rampey RA, Bartel B. Multiple facets of *Arabidopsis* seedling development require indole-3-butyric acid-derived auxin. Plant Cell. 2011; 23:984–999. [PubMed: 21406624]

Toyama R, Mukai S, Itagaki A, Tamura S, Shimozawa N, Suzuki Y, Kondo N, Wanders RJ, Fujiki Y. Isolation, characterization and mutation analysis of *PEX13*-defective Chinese hamster ovary cell mutants. Hum Mol Genet. 1999; 8:1673–1681. [PubMed: 10441330]

Walton PA, Hill PE, Subramani S. Import of stably folded proteins into peroxisomes. Mol Biol Cell. 1995; 6:675–683. [PubMed: 7579687]

Waterham HR, Ebberink MS. Genetics and molecular basis of human peroxisome biogenesis disorders. Biochim Biophys Acta. 2012; 1822:1430–1441. [PubMed: 22871920]

Williams C, Distel B. Pex13p: docking or cargo handling protein? Biochim Biophys Acta. 2006; 1763:1585–1591. [PubMed: 17056133]

Woodward AW, Bartel B. The *Arabidopsis* peroxisomal targeting signal type 2 receptor PEX7 is necessary for peroxisome function and dependent on PEX5. Mol Biol Cell. 2005; 16:573–583. [PubMed: 15548601]

Zolman BK, Bartel B. An *Arabidopsis* indole-3-butyric acid-response mutant defective in PEROXIN6, an apparent ATPase implicated in peroxisomal function. Proc Natl Acad Sci USA. 2004; 101:1786–1791. [PubMed: 14745029]

Zolman BK, Yoder A, Bartel B. Genetic analysis of indole-3-butyric acid responses in *Arabidopsis thaliana* reveals four mutant classes. Genetics. 2000; 156:1323–1337. [PubMed: 11063705]

Zolman BK, Monroe-Augustus M, Thompson B, Hawes JW, Krukenberg KA, Matsuda SPT, Bartel B. *chy1*, an *Arabidopsis* mutant with impaired β-oxidation, is defective in a peroxisomal β-hydroxyisobutyryl-CoA hydrolase. J Biol Chem. 2001a; 276:31037–31046. [PubMed: 11404361]

Zolman BK, Silva ID, Bartel B. The *Arabidopsis pxa1* mutant is defective in an ATP-binding cassette transporter-like protein required for peroxisomal fatty acid β-oxidation. Plant Physiol. 2001b; 127:1266–1278. [PubMed: 11706205]

Zolman BK, Monroe-Augustus M, Silva ID, Bartel B. Identification and functional characterization of *Arabidopsis* PER-OXIN4 and the interacting protein PEROXIN22. Plant Cell. 2005; 17:3422–3435. [PubMed: 16272432]

Zolman BK, Nyberg M, Bartel B. IBR3, a novel peroxisomal acyl-CoA dehydrogenase-like protein required for indole-3-butyric acid response. Plant Mol Biol. 2007; 64:59–72. [PubMed: 17277896]

Zolman BK, Martinez N, Millius A, Adham AR, Bartel B. Identification and characterization of *Arabidopsis* indole-3-butyric acid response mutants defective in novel peroxisomal enzymes. Genetics. 2008; 180:237–251. [PubMed: 18725356]

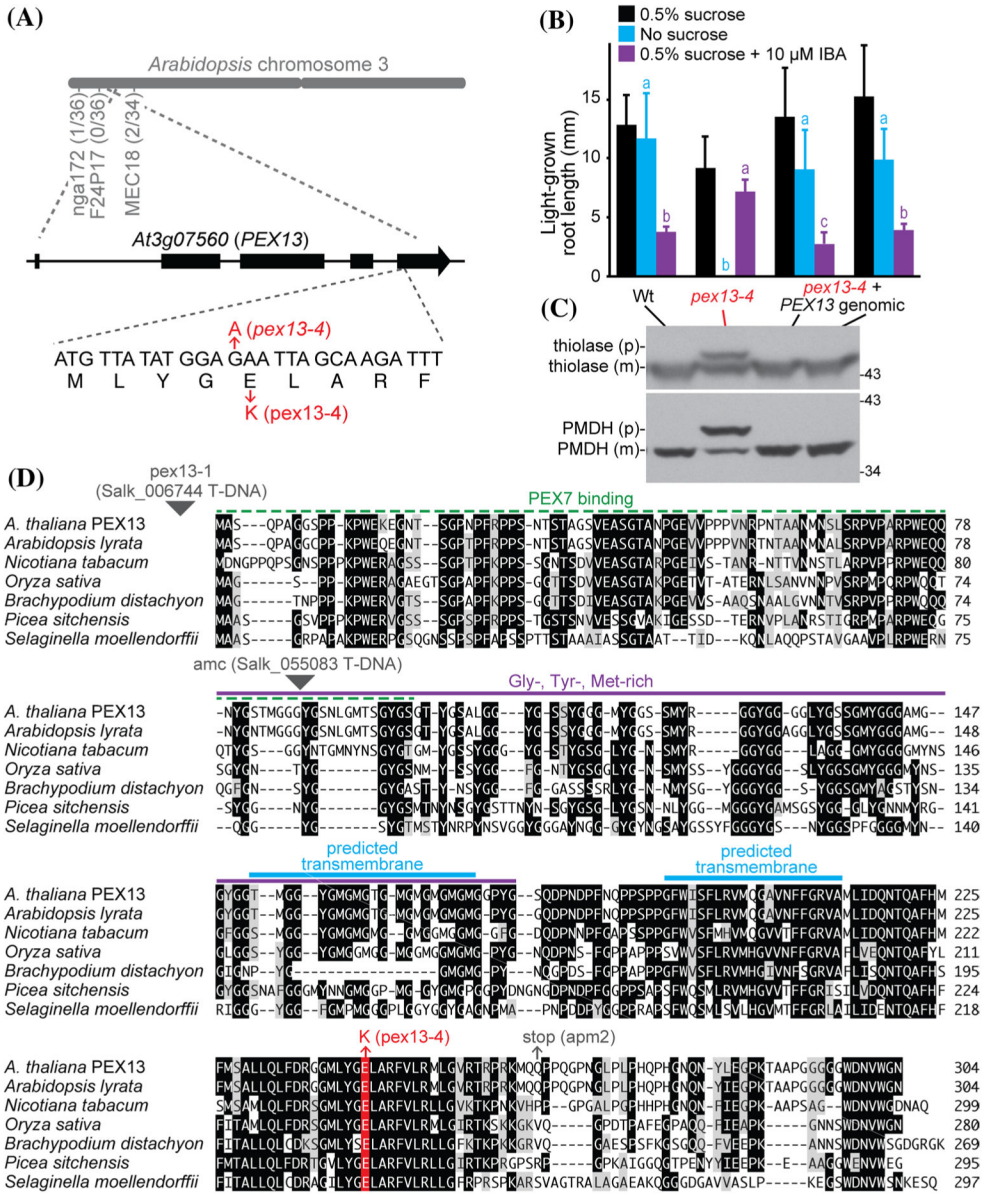

Fig. 1.

Identification of *pex13-4*. **a** The causal mutation in a sucrose-dependent, IBA-resistant mutant was localized using recombination mapping to an interval including *PEX13* (*At3g07560*), which encodes a receptor docking-complex peroxin. The *pex13-4* C-to-T mutation causes a Glu243-to-Lys missense substitution. **b** Expression of wild-type *PEX13* rescues *pex13-4* sucrose dependence and IBA resistance. *Bars* show mean root lengths + SDs ($n \geq 13$) of 8-day-old wild type, *pex13-4*, and two independent lines expressing wild-type *PEX13* genomic clones (pMDC100-*PEX13*) in the *pex13-4* background grown under yellow light on media with or without 0.5 % sucrose or with 0.5 % sucrose supplemented with 10 µM IBA. *Different letters* above bars designate significantly different mean lengths compared to other lines grown on a particular medium (ANOVA, $P < 0.001$). **c** *PEX13* expression rescues *pex13-4* PTS2-processing defects. Lines described in panel B were

grown for 4 days in the light on medium supplemented with 0.5 % sucrose and then processed for immunoblotting. The immunoblot was probed with antibodies to monitor processing of thiolase and PMDH, which are synthesized as precursors (p) that are processed in the peroxisome to mature (m) forms lacking the PTS2 region. Positions of molecular mass markers (in kDa) are shown on the *right*. **d** The *pex13-4* mutation disrupts a residue in a C-terminal domain that is conserved in PEX13 homologs from plants, which were aligned using the MegAlign program (DNAStar) and the Clustal W method. Amino acid residues identical in at least four sequences are boxed in black; chemically similar residues in at least four sequences are boxed in gray. The sites of previously described *Arabidopsis pex13* mutations are shown above the alignment. *Arabidopsis* PEX13 has an N-terminal PEX7-binding region (Mano et al. 2006), a central Gly-, Tyr-, and Met-rich region, and two predicted transmembrane domains. The PEX13 C-terminal region contains an SH3 domain in mammals and fungi (Williams and Distel 2006)

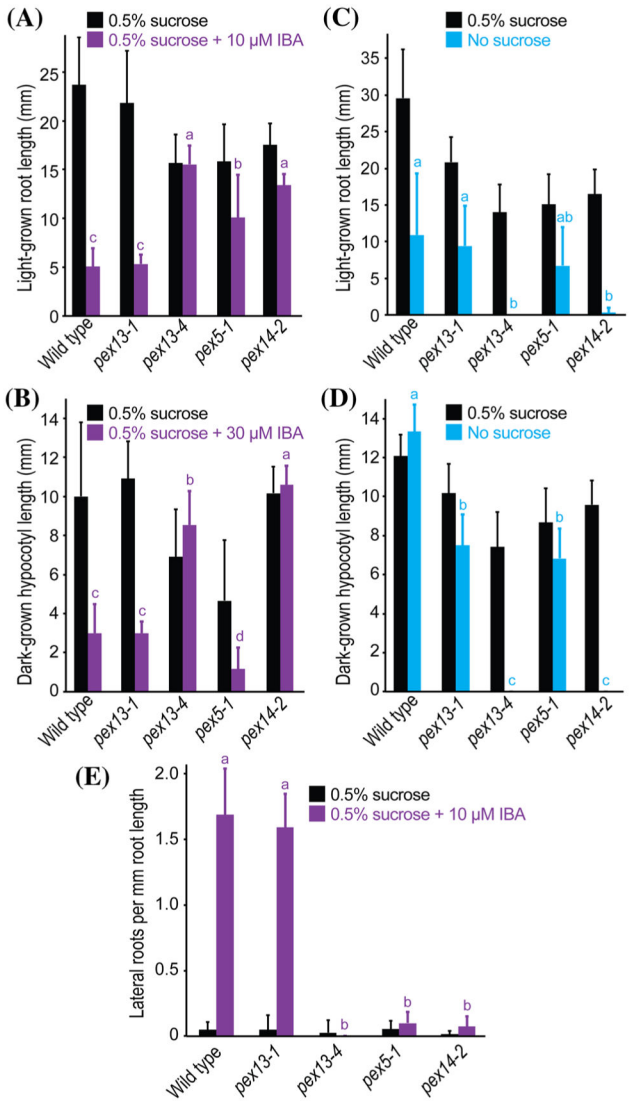

Fig. 2.

pex13-4 seedlings are IBA resistant and sucrose dependent. **a** *pex13-4* is resistant to the inhibitory effects of IBA on root elongation. Seedlings were grown on the indicated media for 8 days under continuous yellow light. **b** *pex13-4* is resistant to the inhibitory effects of IBA on hypocotyl elongation. Stratified seeds were plated on the indicated media and incubated under yellow light for 1 day followed by 4 days in darkness. **c** *pex13-4* seedlings require exogenous sucrose for development in the light. Seedlings were grown on the indicated media for 8 days under continuous yellow light. **d** *pex13-4* seedlings require exogenous sucrose for development in darkness. Stratified seeds were allowed to germinate for 2 days in liquid PN under white light before plating on solidified medium, growing 1 day under white light, and transferring to the dark for 4 days. **e** *pex13-4* is resistant to IBA-induced lateral root proliferation. 4-day-old light-grown seedlings were transferred to the indicated media and incubated for an additional 4 days. *Bars* show means plus SD ($n \geq 10$).

Different letters above bars designate significantly different mean lengths compared to other lines grown on a particular medium (ANOVA, $P < 0.001$)

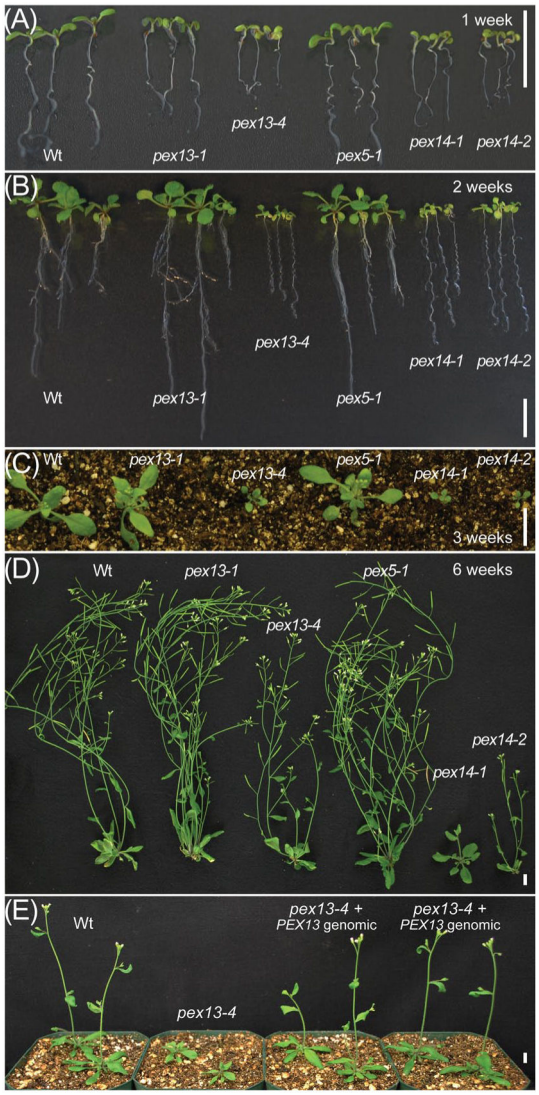

Fig. 3.

pex13-4 plants display delayed development. Plants were grown under continuous light on sucrose-supplemented medium for 2 weeks (**a**, **b**) before transfer to soil (**c**). *pex13-4* seedlings are smaller than wild type and pale green (**a**, **b**), but eventually produce fertile adult plants (**d**). *pex13-4* growth defects are rescued by transformation with a genomic *PEX13* construct (**e**). Wild type, *pex13-4*, and two independent lines expressing wild-type *PEX13* (pMDC100-*PEX13*) in the *pex13-4* background were grown under continuous light on sucrose-supplemented medium for 24 days before transfer to soil and growth for an additional 10 days. Scale bars = 1 cm

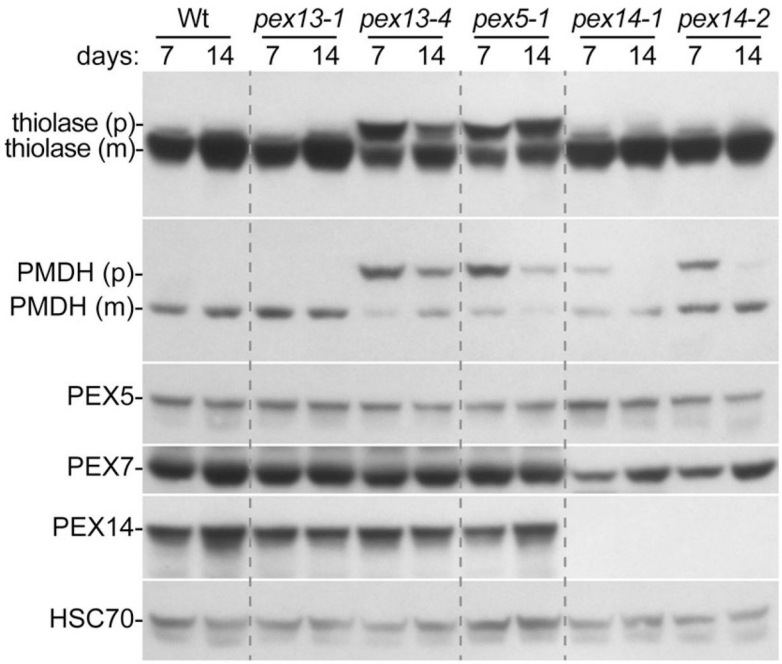

Fig. 4.

pex13-4 seedlings display severe defects in processing PTS2 proteins and accumulate normal PEX5, PEX7, and PEX14 levels. Immunoblots of extracts from 7- and 14-day-old light-grown seedlings were serially probed with the indicated antibodies to monitor peroxin levels and processing of thiolase and PMDH, which are synthesized as precursors (p) that are processed in the peroxisome to mature (m) forms lacking the PTS2 region. HSC70 was used to monitor protein loading

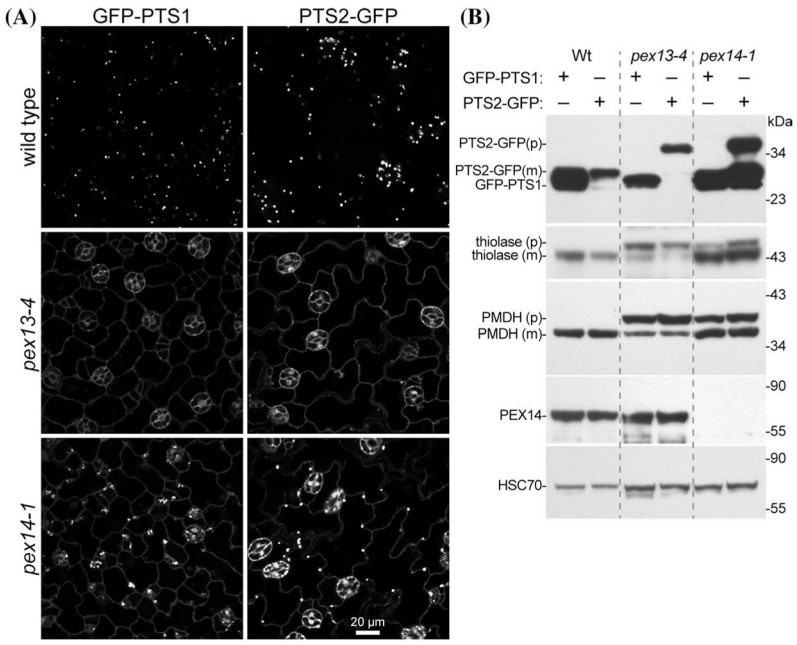

Fig. 5.

pex13-4 mislocalizes PTS1 and PTS2 matrix proteins. **a** Wild-type seedlings display punctate fluorescence typical of peroxisomal localization, *pex13-4* displays primarily cytosolic fluorescence, and *pex14-1* displays a mixture of punctate and cytosolic fluorescence. Cotyledon epidermal cells of 5-day-old light-grown wild-type, *pex13-4*, and *pex14-1* seedlings expressing *35S:GFP-PTS1* or *35S:PTS2-GFP* were imaged for GFP fluorescence using confocal microscopy. The large central vacuole in epidermal cells causes the cytosol to be concentrated at the cell margins. Scale bar = 20 μm. **b** *pex13-4* exhibits a nearly complete defect in processing PTS2–GFP. Immunoblots of extracts from 5-day-old light-grown seedlings were serially probed with antibodies to GFP, thiolase, and PMDH to monitor PTS2 processing from the precursor (p) to the mature form (m) lacking the PTS2 region. HSC70 was used to monitor protein loading

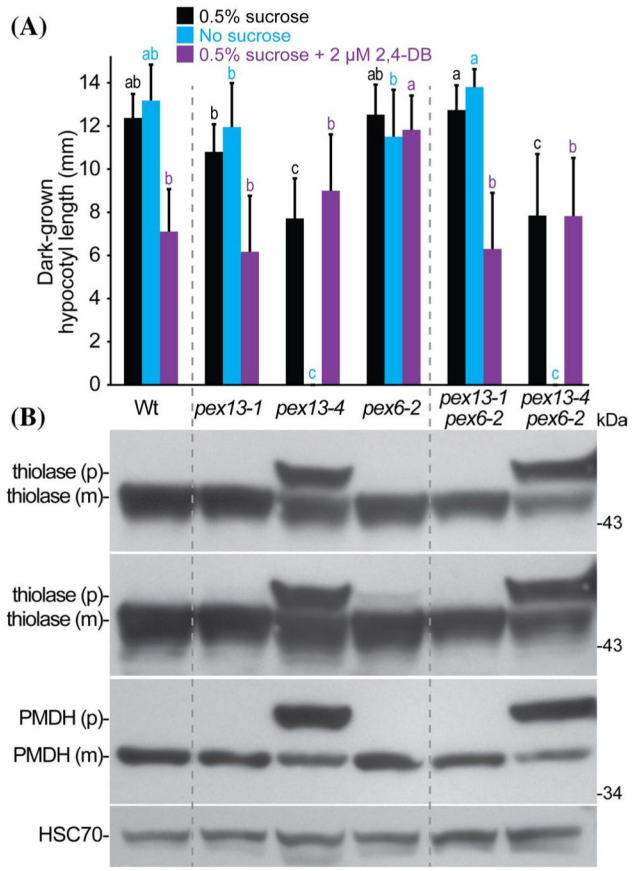

Fig. 6.

pex6-2 defects are enhanced by *pex13-4* and suppressed by *pex13-1*. **a** *pex13-1* suppresses the 2,4-DB resistance of *pex6-2; pex13-4 pex6-2* resembles *pex13-4. Bars* show mean hypocotyl lengths plus SD ($n \geq 13$). Seeds were stratified for 1 day, allowed to germinate in the absence of hormone under yellow light for 1 day, plated on the indicated media and returned to yellow light for 1 day, and then placed in darkness for 4 days. *Different letters* above bars designate significantly different mean lengths compared to other lines grown on a particular medium (ANOVA, $P < 0.001$). **b** Immunoblots of extracts from 5-day-old light-grown seedlings were serially probed with antibodies to the indicated proteins to monitor processing of thiolase and PMDH, which are synthesized as precursors (p) that are processed in the peroxisome to a mature form (m) lacking the PTS2 region. Two exposures of the thiolase immunoblot are shown to allow visualization of the slightly enhanced thiolase-processing defect in *pex13-4 pex6-2* compared to *pex13-4* (*top panel*) and the slight thiolase-processing defect in *pex6-2* (*second panel*) that is suppressed in *pex13-1 pex6-2*. HSC70 was used to monitor protein loading. Positions of molecular mass markers (in kDa) are shown on the *right*

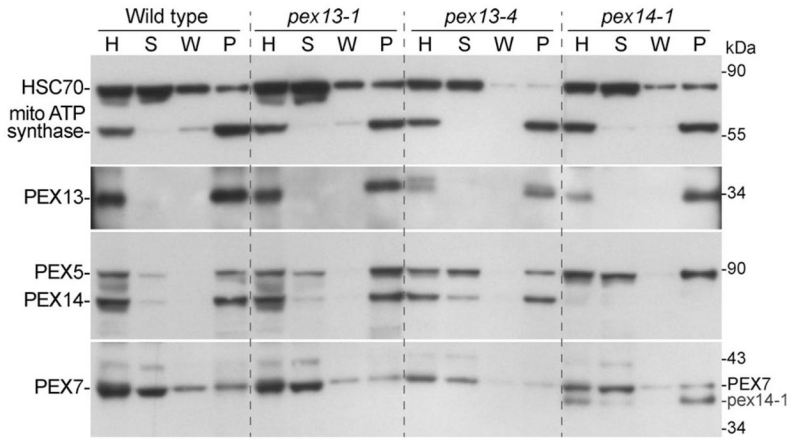

Fig. 7.

PEX5 is less organelle-associated in *pex13-4*. Whole-seedling homogenates from 8-day-old light-grown seedlings were separated by centrifugation into soluble and organellar pellet fractions. For each sample, equal volumes of total homogenate (H), soluble fraction (S), wash (W), and pellet fraction (P) were separated using SDS-PAGE and processed for sequential immunoblotting using the indicated antibodies. The mitochondrial membrane complex V subunit α (mito ATP synthase) and cytosolic HSC70 were used as organellar and cytosolic controls, respectively. Positions of molecular markers (in kDa) are indicated on the *right*. The position of the truncated pex14-1 protein product from an earlier probing of the membrane is marked in the anti-PEX7 panel

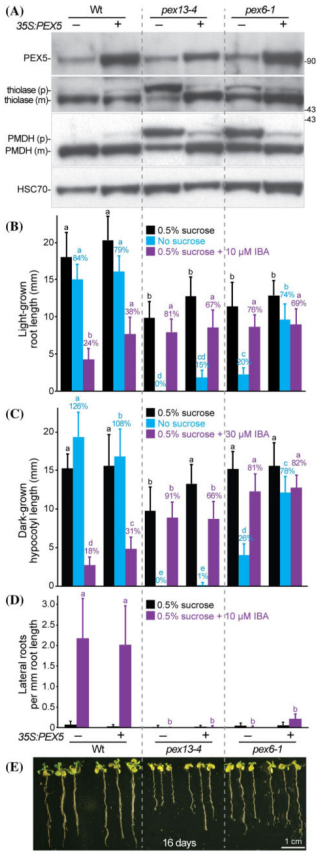

Fig. 8.

Overexpressing PEX5 partially ameliorates a subset of *pex13-4* defects. **a** Overexpressing PEX5 partially suppresses *pex13-4* PTS2-processing defects. Immunoblots of extracts prepared from 6-day-old light-grown seedlings were serially probed with antibodies to the indicated proteins to monitor PEX5 levels and processing of thiolase and PMDH, which are synthesized as precursors (p) that are processed to a mature form (m) lacking the PTS2 region in the peroxisome. HSC70 was used to monitor protein loading. Positions of molecular mass markers (in kDa) are shown on the *right*. **b** Overexpressing PEX5 slightly suppresses *pex13-4* sucrose dependence in the light. *Bars* show mean root lengths plus SD ($n \geq 14$) of 8-day-old light-grown seedlings grown on the indicated media. *Percentages* above bars are relative lengths compared to the 0.5 % sucrose control for each line. *Different letters* above bars designate significantly different mean lengths compared to other lines grown on a given medium (ANOVA, $P < 0.001$). **c** Overexpressing PEX5 slightly suppresses *pex13-4* IBA resistance in the dark. *Bars* show mean hypocotyl lengths plus SD ($n \geq 16$) of dark-grown wild-type, *pex13-4*, and *pex6-1* seedlings without (−) or with (+) the *35S:PEX5* construct. *Percentages* above bars are relative lengths compared to the 0.5 % sucrose control for each line. *Different letters* above bars designate significantly different mean lengths compared to other lines grown on a given medium (ANOVA, $P < 0.001$). Seeds were stratified for 1 day, plated on the indicated media, incubated under yellow light for 1 day, and then placed in darkness for 5 days. **d** Overexpressing PEX5 does not affect *pex13-4* IBA resistance in lateral root production. 4-day-old light-grown seedlings were

transferred to the indicated media and incubated for an additional 4 days. *Bars* show mean numbers of lateral roots/mm root length plus SD ($n \geq 12$). *Different letters* above bars designate significantly different mean lengths compared to other lines grown on a particular medium (ANOVA, $P < 0.001$). **e** Overexpressing PEX5 slightly suppresses *pex13-4* growth defects. Seedlings were grown in the light on sucrose-supplemented medium and removed from the agar for photography after 16 days. Scale bar = 1 cm